Eur. Phys. J. D **31**, 121–129 (2004)
DOI: 10.1140/epjd/e2004-00112-5

THE EUROPEAN PHYSICAL JOURNAL D

Isotropic quantum beats

I. Pulsed pump-probe detection

P. Johansson[1], I.E. Mazets[2], O.S. Vasyutinskii[2], and T. Hansson[1,a]

[1] Stockholm University, AlbaNova University Center, Department of Physics, 106 91 Stockholm, Sweden
[2] Ioffe Physico-Technical Institute, Russian Academy of Sciences, 194021 St. Petersburg, Russia

Received 19 April 2004 / Received in final form 23 June 2004
Published online 31 August 2004 –

Abstract. Previous theoretical work reviewed in [E.B. Alexandrov et al. *Interference of atomic states* (Springer, 1993)] has questioned the existence of isotropic quantum beats in atoms. The present work addresses this issue in dedicated experiments involving a pulsed pump-probe detection scheme. The thus obtained results show clear evidence of isotropic quantum beats for which a physical interpretation is given within the coupled-uncoupled state formalism. We suggest that assumptions made in the earlier theoretical work with respect to the structure of the light field make the predictions applicable to scattering only of single photons by atoms and not to scattering of the classical-like light pulses used in ordinary experiments.

PACS. 42.50.Ct Quantum description of interaction of light and matter; related experiments – 42.50.Md Optical transient phenomena: quantum beats, photon echo, free-induction decay, dephasings and revivals, optical nutation, and self-induced transparency

1 Introduction

The phenomenon of atomic quantum beats is now known since more than forty years [1,2] and being generalized to molecules [3] and condensed matter [4] it has found many applications to study microscopic properties of ordinary matter. In itself, atomic quantum beating represents a general and fundamental principle of modern physics, that of interference within an impulsively created coherent superposition of quantum eigenstates. Such superposition states in atoms may be achieved in various ways, e.g., by fast collisions in atomic beam-foil experiments [5], by pulsed electron beam-atom collisions [6] or as considered here by exposure to short light pulses [1]. The latter method is today routinely used [7] to create such diverse entities as quantum wavepackets built-up of electronic Rydberg states in atoms or rovibrational molecular states, both kinds suggested as media for quantum computing.

Evidently, then, in addition to the fundamental aspects important contemporary scientific methods and technological advances rely on phenomena linked in theory to quantum beats, in particular atomic ones. Below, we will briefly restate the standard theoretical formulation of atomic quantum beats [8], which treats the light-atom interaction within the electric-dipole approximation and only takes into account lowest-order interaction.

The standard description has been challenged, however. In a series of publications [9–11] summarized in reference [8] Khvostenko and Chaika (KC) have suggested that a particular kind of atomic quantum beating (and level-crossing), that between states with all identical angular momentum quantum numbers but different principal quantum numbers, while being allowed in the standard theory, would be disallowed when higher-order photon-atom interactions through the vacuum are taken into account. In reference [12], moreover, the very general claim is made that "... for [atomic] states with all equal angular momenta the signals of level crossing... and free beats... are exactly zero at any observation geometry, i.e., for an arbitrary polarization observed in an arbitrary direction, provided that irradiation and observation are carried out in a wide spectral range". Note that, unlike the well-known quantum beating effects within Zeeman, fine, or hyperfine energy level manifolds in atoms [8], the effect considered by KC is *isotropic*, that is, it does not depend on any light polarisation.

It is important to distinguish between the isotropic electronic quantum beats considered by KC and known beating (revival) effects related to oscillations in radial wavepacket motion in atoms and molecules, see reference [7] for an overall review, which also can be isotropic, for known reasons. Of particular interest here is the experimental study on radial Rydberg electron wavepacket dynamics in calcium atoms by Strehle et al. [13]. For wavepackets, beating effects can be treated quasiclassically, in the referred to specific case as a result of periodical spatial overlap between the ground and excited state

[a] e-mail: tony.hansson@physto.se

wavepackets leading to oscillations in the values of the corresponding transition probabilities.

Contrary to this quasiclassical behavior of Rydberg wavepackets, the KC quantum beating effect [8] considered in this paper is of pure quantum mechanical nature. It appears between two or more quantum states excited by a short pulse and represents a basic quantum mechanical principle of coherent superposition of quantum amplitudes. For low-lying excited states such electronic quantum beats have little similarity with wavepacket motion. For high-lying states, however, the border between these two effects is smooth. For instance, some of the above-mentioned experimental results reported by Strehle et al. [13] can alternatively be treated in terms of the coupled-uncoupled state representation (see Sect. 5.2).

To our best knowledge, the KC prediction, henceforth called the KC conjecture, has not been put to a rigorous experimental test. This is surprising considering its far-reaching fundamental and practical implications. In the present work we address the applicability of the KC conjecture with respect to pulsed light excitation, treated explicitly in references [8,11], in its above-cited general form [12] by pulsed pump-probe spectroscopy. Our experimental results display clear quantum beats of purely radial nature, which shows that the KC conjecture does not apply under these conditions and, hence, the generalized version of the conjecture is invalid. We suggest that this disagreement relates to the assumptions made in the KC theoretical work with respect to the structure of the light field. We also offer a physical interpretation of the observed isotropic quantum beats within the coupled-uncoupled state formalism.

2 Theoretical preliminaries

For reference we outline in this section the standard formulation of atomic quantum beating theory as applied to pump-probe detection. Consider an atom initially in the manifold of its degenerate ground states $|g\rangle$ interacting with two pulsed electromagnetic fields E_{pu} and E_{pr} of duration τ and well-separated in time with a delay $t \gg \tau$. The pump pulse couples the atomic ground state $|g\rangle$ to an intermediate electronic excited state manifold $|\Psi_{int}\rangle$ whereas the subsequent probe pulse acts on the $|\Psi_{int}\rangle \rightarrow |f\rangle$ transition to populate the final state manifold $|f\rangle$. For the sake of argument each transition is here assumed to be a single-photon one.

The general expression for the pump-probe delay time-dependent signal then can be written

$$I(t) \sim \sum_f \left|\langle f| \mathbf{de}_{pr} |\Psi_{int}(t)\rangle\right|^2, \qquad (1)$$

where $\mathbf{d}$ is the probe transition dipole moment and $\mathbf{e}_{pr}$ is the probe light polarization vector.

Choosing $t = 0$ to coincide with the onset of the pump pulse and limiting the treatment to delay times much shorter than the excited state lifetime we have

$$|\Psi_{int}(t)\rangle = \sum_j a_j(\tau) e^{-i\hat{H}_a(t-\tau)/\hbar} |j\rangle, \qquad (2)$$

where $\hat{H}_a$ is the atomic Hamiltonian in the absence of radiation and the coefficients $a_j(\tau)$ describe excitation of the atom from the ground to the intermediate state and can be determined by usual first order perturbation theory.

In the simplest case of a spinless atom the intermediate state eigenvectors $|j\rangle = |n_j L_j M_j\rangle$ where n_j is the main quantum number, L_j the total electronic angular momentum, and M_j the projection of L_j onto the laboratory Z-axis. Similarly, for the initial $|g\rangle$ and final state $|f\rangle$ we have $|n_g L_g M_g\rangle$ and $|n_f L_f M_f\rangle$. The Hamiltonian $\hat{H}_a$ in equation (2) is diagonal in this representation. Assuming equal population of each M_g ground state magnetic sublevel and noting that from the conditions above $t - \tau \approx t$ the pump-probe signal in equation (1) can be rewritten in the general form

$$I(t) \propto \sum_{f,g} \left| \sum_j \langle f| \mathbf{de}^*_{pr} |j\rangle e^{-\frac{i}{\hbar}E_j t} \langle j| \mathbf{de}_{pu} |g\rangle \right|^2. \qquad (3)$$

Here, E_j is the energy of the jth intermediate state whereas $\mathbf{e}_{pu}$ and $\mathbf{e}_{pr}$ is the polarization of the pump and probe photon, respectively. The summation proceeds over all initial, intermediate, and final states involved in the pump-probe process. This generally rather complicated formula contains both time-independent incoherent terms with $j = j'$ and time-dependent coherent terms with $j \neq j'$, the latter ones being responsible for the quantum beating phenomenon. Assuming there is only one initial $|n_g, L_g\rangle$ state and one final $|n_f, L_f\rangle$ state involved and using the Wigner-Eckart theorem [14], equation (3) after summation over all projections M_g, M_j, M'_j, and M_f becomes

$$\begin{aligned} I(t) = C \sum_K \sum_{n_j,n'_j} \sum_{L_j,L'_j} (-1)^{K+L_g+L_f+L_j+L'_j} \\ \times (E_K(\mathbf{e}_{pu}) \cdot E_K(\mathbf{e}_{pr})) \\ \times \left\{ \begin{array}{ccc} L_j & L'_j & K \\ 1 & 1 & L_g \end{array} \right\} \left\{ \begin{array}{ccc} L_j & L'_j & K \\ 1 & 1 & L_f \end{array} \right\} e^{-i\omega_{jj'}t} \\ \times \langle n_f L_f \| \mathbf{d} \| n_j L_j \rangle^* \langle n_f L_f \| \mathbf{d} \| n'_j L'_j \rangle \\ \times \langle n_j L_j \| \mathbf{d} \| n_g L_g \rangle^* \langle n'_j L'_j \| \mathbf{d} \| n_g L_g \rangle. \end{aligned} \qquad (4)$$

The terms within angular braces are reduced dipole moment matrix elements whereas curly braces denote $6j$ symbols. C is a constant and $E_K(\mathbf{e}_{pu}) \cdot E_K(\mathbf{e}_{pr})$ is the scalar product of the irreducible tensors of the pump and probe light polarizations [15]. Defining the pump light polarization to coincide with the laboratory Z-axis and using explicit expressions for the zeroth and the second rank light polarization irreducible tensor from reference [8] one can show that $E_0(\mathbf{e}_{pu}) \cdot E_0(\mathbf{e}_{pr}) = 1/3$ and $E_2(\mathbf{e}_{pu}) \cdot E_2(\mathbf{e}_{pr}) \propto P_2(\cos\Theta)$, where $P_2(\cos\Theta)$ is the second-order Legendre polynomial and Θ is the angle between the pump and the probe polarization vectors.

Note that quantum beats are frequently studied not by detecting absorption of the probe light beam as above, but by detecting polarization of the fluorescence light emitted from intermediate states. The fluorescence signal can still

be successfully described by equation (4), however, with additional phenomenological terms $e^{-\Gamma_j t}$ where Γ_j is the radiative lifetime of the $|j\rangle$ state [3,8].

The index K in equation (4) is limited to the values $\{0, 1, 2\}$ which describe contributions to the absorption signal from the atomic population, orientation, and alignment, respectively. The contribution from the $K = 1$ term vanishes if the pump and the probe laser pulses are both linearly polarized. The $K = 0$ term is isotropic as it does not depend on the polarization of the pump and probe radiation but solely on the total number of atoms in the $|j\rangle$ manifold. The non-zero K terms, on the other hand, are anisotropic as they depend on Θ. These terms originate in the spatial anisotropy of the atomic angular momenta L_j and L'_j.

The value $\omega_{jj'} = (E_j - E'_j)/\hbar$ in equation (4) is the difference between frequencies of the intermediate quantum states and the corresponding time-dependent exponent is the origin of the quantum beats. It is easy to show from the symmetry properties of the $6j$ symbols in equation (4) that in case $L_j \neq L'_j$ the value of K must differ from zero. Therefore, no isotropic quantum beats can exist in this case. This result can be generalized for more complicated atomic wave functions taking into account spin-orbit and hyperfine interactions and containing the set of quantum numbers n_j, L_j, S (electron spin), J_j (total electron angular momentum), I (nuclear spin), and F_j (total angular momentum). It can be shown (see, e.g., Ref. [8]) that if $L_j \neq L'_j$, or $J_j \neq J'_j$, or $F_j \neq F'_j$, then no isotropic quantum beats can exist.

If instead $L_j = L'_j$ but $n_j \neq n'_j$, equation (4) predicts non-zero time-dependent contribution from the $K = 0$ term leading to isotropic quantum beating where the beat amplitude does not depend on the pump and probe light polarization. As far as we know, no experimental observation of this effect has been reported until now. The prediction may look surprising, because in the general case of two arbitrary quantum states this kind of beats might result only from oscillation of the excited state total atomic concentration [11]. Khvostenko and Chaika [9–11] therefore argued that equation (4) based on the first order perturbation theory is not sufficient in case $L_j = L'_j$ and $n_j \neq n'_j$ and that taking into account higher orders of the perturbation series cancels the isotropic quantum beating.

3 Experimental

3.1 Pump-probe scheme

The atomic system employed for the experiments is the spectroscopically well-studied [16,17], nonetheleast by pulsed pump-probe spectroscopy [13], ^{40}Ca atom. It has a non-degenerate ^{1}S$_0$ ground state and lacks nuclear spin which ensures both the absence of perturbing hyperfine interaction and that the superposition state is not obscured by statistical averaging over initial quantum states related to angular momentum projections.

As described just below, the pump pulse excited levels with $n \approx 15$ in a two-photon transition. Depending on light polarization, then, there was one or two of the $(4sns)\,^1$S$_0$ and $(4snd)\,^1$D$_2$ manifolds with $m_J = 0$ or 2 addressed at a time. The ^{1}S$_0$ manifold appears to be unperturbed in the applicable n range while some ^{1}D$_2$ states, most notably $4s13d$, are perturbed by spin-orbit interactions [16].

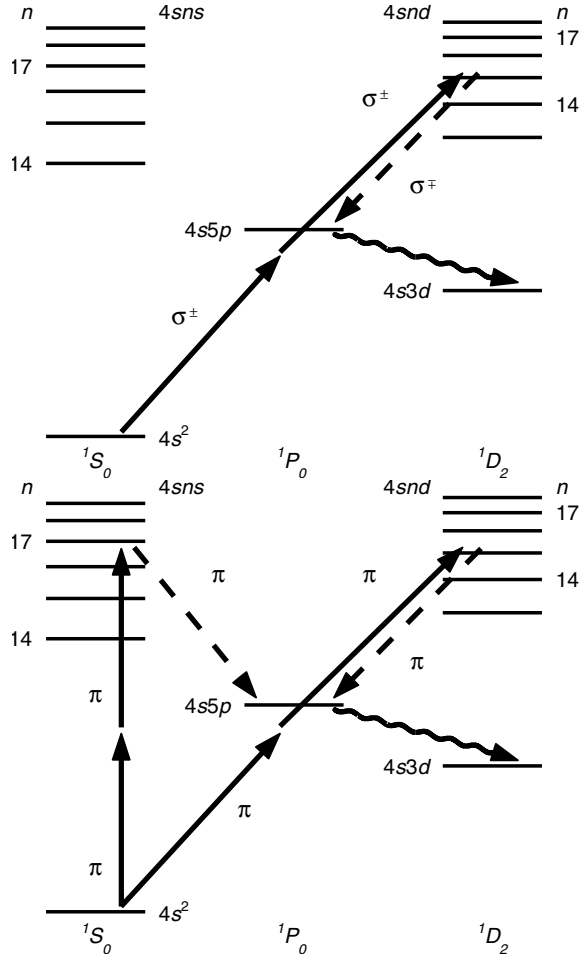

Fig. 1. Pump-probe scheme. Top: circular light polarization; Bottom: linear polarization.

Figure 1 illustrates our pump-probe scheme. It was for all purposes advantageous to address as low-lying as possible atomic levels in the excited superposition state. The lower n limit is determined by the spectral bandwidth of the employed light pulses, in our case 120 and 150 cm^{-1}, respectively, corresponding to $n \approx 15$, if only a small number of states is to be excited. In calcium, however, these levels are inconveniently high in energy for a one-photon excitation scheme. We therefore used instead a non-resonant two-photon pump transition at 411 nm.

A circularly polarized $\sigma^{\pm}$ pump pulse, Figure 1 (top), thus addressed only $m_J = \pm 2$ states in the $(4snd)\,^1$D$_2$ manifold. With linear light polarization, on the other hand, $m_J = 0$ states in both the $(4sns)\,^1$S$_0$ and $(4snd)\,^1$D$_2$ manifolds were accessed, Figure 1 (bottom). In either case, the time evolution of the pumped state was mapped out by a time-delayed probe pulse that stimulated a downward transition to the $(4s5p)\,^1$P$^o_1$ level, a process

which was monitored by detecting, to avoid contribution from cascade processes, early fluorescence intensity of the $(4s5p)\,^1\mathrm{P}_1^o \rightarrow (4s3d)\,^1\mathrm{D}_2$ line. For $\sigma^{\pm}$ polarized pump light, a $\sigma^{\mp}$ probe was used, resulting in an overall scheme that below is denoted $[\sigma^+]^2\sigma^-$ or, vice versa, $[\sigma^-]^2\sigma^+$ whereas for a π polarized pump the probe was π polarized either parallel ($\pi^2 \parallel \pi$) or perpendicular ($\pi^2 \perp \pi$) to the pump.

The theoretical expressions in the previous section were derived for a 1+1 type pump-probe scheme and hence cannot be directly used for our $2+1$ scheme. The general equations (1) and (2) are still valid, however, where the coefficients $a_j(\tau)$ now describe two-photon excitation from the atomic ground state and can be calculated by standard second order time-dependent perturbation theory. Introducing virtual atomic states $|v\rangle$ and summing over the projections of all angular momenta the expression for the light absorption intensity $I(t)$ after some simplifications becomes

$$I(t) = C \sum_{k_1,k_2,k_3} (-1)^{k_2+k_3} \sqrt{(2k_2+1)(2k_3+1)} S_{k_3}^{k_1 k_2}(t) \times \left\{ [E_{k_1}(\mathbf{e}_1) \otimes E_{k_2}(\mathbf{e}_2)]_{k_3} \cdot E_{k_3}(\mathbf{e}_3) \right\}. \quad (5)$$

Here $k_j = 0, 1, 2$ ($j = 1, 2, 3$) are ranks of the first, second, and the third photon polarization tensor, respectively, and the third photon is assumed to be the probe one. The product within curly brackets in equation (5) is

$$[E_{k_1}(\mathbf{e}_1) \otimes E_{k_2}(\mathbf{e}_2)]_{k_3} \cdot E_{k_3}(\mathbf{e}_3) = \sum_{\alpha,\beta,\gamma} (-1)^{\gamma} C_{k_1\,\alpha\;k_2\,\beta}^{k_3\,-\gamma} \times E_{k_1,\alpha}(\mathbf{e}_1) E_{k_2,\beta}(\mathbf{e}_2) E_{k_3,\gamma}(\mathbf{e}_3), \quad (6)$$

where $C_{k_1\,\alpha\;k_2\,\beta}^{k_3\,-\gamma}$ is a Clebsch-Gordan coefficient [14] and

$$S_{k_3}^{k_1 k_2}(t) = \sum_{L_j,L_j'} \sum_{L_v,L_v'} \sum_{n_v,n_v'} \sum_{n_j,n_j'} (-1)^{L_g+L_j'+L_v'+L_f+1} \times \begin{Bmatrix} 1 & 1 & k_3 \\ L_j' & L_j & L_f \end{Bmatrix} \begin{Bmatrix} 1 & 1 & k_1 \\ L_v' & L_v & L_g \end{Bmatrix} \times \begin{Bmatrix} L_v & 1 & L_j \\ L_v' & 1 & L_j' \\ k_1 & k_2 & k_3 \end{Bmatrix} e^{-i\omega_{jj'}t} \times S(n_g L_g, n_v L_v, n_v' L_v', n_j L_j, n_j' L_j', n_f L_f). \quad (7)$$

The factor $S(n_g L_g, n_v L_v, n_v' L_v', n_j L_j, n_j' L_j', n_f L_f)$ contains reduced matrix elements and the energy denominator of second order perturbation theory:

$$\begin{aligned} S(\gamma_g j_g, \gamma_v j_v, \gamma_v' j_v', \gamma_j j_j, \gamma_j' j_j', \gamma_f j_f) = {} & \\ & \langle n_f L_f \| d^{(3)} \| n_j' L_j' \rangle \langle n_f L_f \| d^{(3)} \| n_j L_j \rangle^* \\ & \times \{ (E_{gv} - h\nu - i\Gamma_v/2)(E_{v'g} - h\nu + i\Gamma_v/2) \}^{-1} \\ & \times \langle n_j' L_j' \| d^{(2)} \| n_v L_v \rangle \langle n_j L_j \| d^{(2)} \| n_v L_v \rangle^* \\ & \times \langle n_v' L_v' \| d^{(1)} \| n_g L_g \rangle \langle n_v L_v \| d^{(1)} \| n_g L_g \rangle^*. \end{aligned} \quad (8)$$

Although the expression for the quantum beating in equation (5) is more complicated than that in equation (4) it retains the same main features of the phenomenon. This can be clearly seen assuming the polarization of the pump light $\mathbf{e}_1 = \mathbf{e}_2 = \mathbf{e}_{pu}$ is parallel to the laboratory Z-axis, which restricts the values of all the projections α, β, and γ in equation (6) to zero. The contribution from all $k_3 = 0$ terms in equation (5) describes the isotropic quantum beats as the product (6) does not depend on the relative direction of the $\mathbf{e}_{pu}$ and the $\mathbf{e}_3 = \mathbf{e}_{pr}$ polarization vectors. The anisotropic quantum beats, on the other hand, are described by the $k_3 = 2$ terms which do depend on the relative polarization of the pump and probe light as $\left\{ [E_{k_1}(\mathbf{e}_{pu}) \otimes E_{k_2}(\mathbf{e}_{pu})]_{k_3} \cdot E_2(\mathbf{e}_{pr}) \right\} \propto P_2(\cos\Theta)$. Also, as can be seen from the symmetry properties of the $6j$ symbol in equation (7), in case $L_j \neq L_j'$ all $k_3 = 0$ terms vanish and thus only the anisotropic quantum beats can exist. If $L_j = L_j'$ both isotropic ($k_3 = 0$) and anisotropic ($k_3 = 2$) quantum beats can exist. Thus, the 2+1 quantum beating signal in equation (5) exhibits the same features as the $1 + 1$ signal in equation (4).

3.2 Set-up

In brief, the experimental set-up comprised a femtosecond laser system in a standard pump-probe configuration with polarization control coupled to a heat-pipe oven for sample generation. Fluorescence light emitted from the oven was spectrally decomposed and detected by time-gated photon counting, a procedure that was repeated for a range of pump-probe delays.

The required ultrashort pump and probe pulses at about 411 and 835 nm, respectively, were generated in several steps. The output pulse of a femtosecond laser system (CPA2001, Clark-MXR) was split in two and used to synchronously pump two identical optical parametric amplifiers (TOPAS-4, Light Conversion). The pump pulse was generated by nonlinear mixing in BBO crystals to obtain the third harmonic of the TOPAS' signal pulse. The probe pulse was obtained similarly by frequency doubling of the idler pulse and its timing with respect to the pump pulse was controlled by a mechanical delay stage with 1 μm path length resolution.

The final light pulses had bandwidths of 120 (pump) and 150 cm^{-1} (probe) and the overall time-resolution after pulse compression was characterized by a Gaussian cross-correlation width of about 150 fs in a SiC photodiode (JEC1, Laser Components) [18] just before the oven entrance window. The pulse fluence of the pump and probe thus obtained was at the oven 2−5 μJ. The polarization state of the pulses was always purer than 100:1 and could be controlled by various waveplate combinations. With linear pulse polarization a broadband $\lambda/2$ waveplate (ACWD-400-700-10-2, CVI) was inserted into the pump beam. Circularly polarized pulses were obtained by inserting a variable Berek compensator (5540, New Focus) in each beam. Finally, the pulses were focused by $f = +50$ cm plano-convex lenses and the focii were spatially overlapped

in the center of the heat-pipe oven after entering through a 3.0 mm BK7 window (Melles Griot).

The gaseous calcium atom sample was generated by putting grains of the metal (natural isotope mixture) in the center of a ceramic heat-pipe oven and heating to around 550 °C in the presence of 0.1 mbar of argon buffer gas. The buffer pressure was balanced such as to maximize the detected fluorescence intensity, which increases with pressure, while avoiding substantial dephasing of the atomic superpositions within the timescale of the experiment. Thus, the applied buffer gas pressure was significantly lower than the in the order of 10 mbar used in standard applications, at which pressures we saw clear quenching of the atomic beats. The oven was resistively AC heated through a 0.75 mm diameter wolfram wire singly wound around the ∅ 3 cm cylindrical oven. A 50 Hz current of 16 A was required to maintain the operation temperature.

Fluorescence light from the sample was collected in the backward direction with a $f = +30$ cm lens close to the short-pulse entrance window. This light was spectrally (OG 570, Schott) and spatially filtered and imaged onto a 20 cm monochromator (H 20 IR, Jobin-Yvon) set at 672.5 nm with a FWHM bandpass of 4 nm to monitor the $(4s5p)\,{}^1\mathrm{P}_1^o \rightarrow (4s3d)\,{}^1\mathrm{D}_2$ transition. The detection was effected by a photomultiplier tube (R928, Hamamatsu) operated in photon counting mode and connected to a gated photon counter (SR400, Stanford Research). A time gate was applied to discriminate against background photons from cascade processes by utilising the fact that the cascade process is much slower than the decay of the population induced by the probe pulse. Thus, the gate was delayed about 10 ns with respect to the arrival of the pump pulse to avoid scattered pump light and then set to cover the following 80 ns of the transient fluorescence light. For each pump-probe delay the signal was summed over 2000 laser cycles. A similar set-up was used to simultaneously record the excited atomic density in the oven by collecting fluorescence light in the forward direction and setting the monochromator to monitor mainly the $(4s15s - 4s18s)\,{}^1\mathrm{S}_0$ and $(4s14d - 4s18d)\,{}^1\mathrm{D}_2$ to $(4s4p)\,{}^1\mathrm{P}_1^o$ transitions at around 390 nm.

4 Results

The primary data from the experiments were pump-probe delay time traces. In these, zero delay time corresponds to pump and probe pulses arriving simultaneously to the sample, while negative time means the probe pulse arrives prior to the pump. In the latter case we recorded only background counts without noticeable pump-probe contribution.

Interpretation of the data is most easily done in the frequency domain and the power spectrum of each trace, defined as the absolute square of the corresponding fast Fourier transform, is given. The notation of the peak assignments in these graphs are of the form *nx-my* which denotes a beat frequency corresponding to the energy difference between the $4snx$ and $4smy$ levels. In the assignment procedure we have in view of its vanishing intensity in the two-photon excitation spectrum [16] excluded the possibility of any combinations involving the $4s13d$ level. It should be noted that we to obtain the power spectra only include positive delay times corresponding to well-separated pulses and subtract a constant background to have a signal oscillating around approximately zero level.

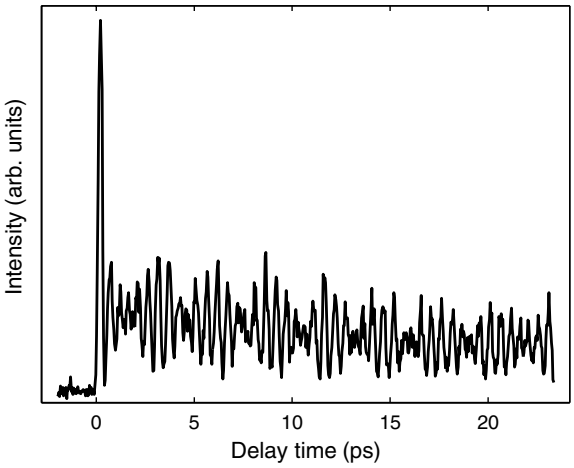

Fig. 2. Time trace obtained with the $[\sigma^+]^2\sigma^-$ scheme and $\lambda_{pu} = 410$ nm and $\lambda_{pr} = 833$ nm.

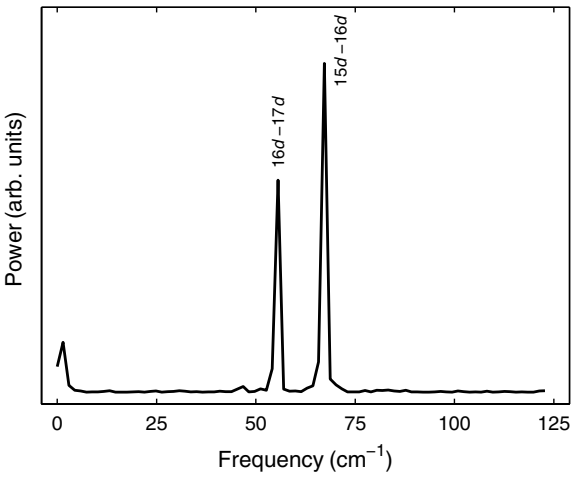

Fig. 3. Power spectrum of the $[\sigma^+]^2\sigma^-$ trace in Figure 2.

4.1 Circular light polarization

Figure 2 displays a time trace obtained with the $[\sigma^+]^2\sigma^-$ pump-probe scheme. Its outstanding feature is the seemingly simple quantum beat structure. This simplicity is obvious in the corresponding power spectrum in Figure 3 which exhibits only two significant peaks. Importantly, these peaks correspond to beat frequencies involving only $4snd$ levels, that is, they are of pure *d-d* type.

Two more traits of the time trace deserving mentioning are the sharp strong peak at around zero time delay and the slow overall decay of the signal level.

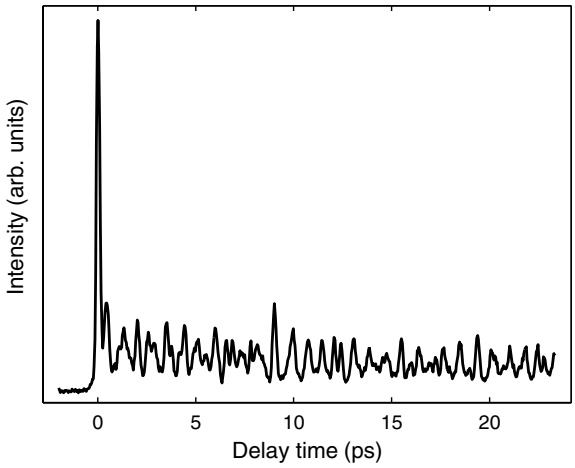

Fig. 4. Time trace obtained with the $\pi^2 \parallel \pi$ scheme and $\lambda_{pu} = 411\,\text{nm}$ and $\lambda_{pr} = 837\,\text{nm}$.

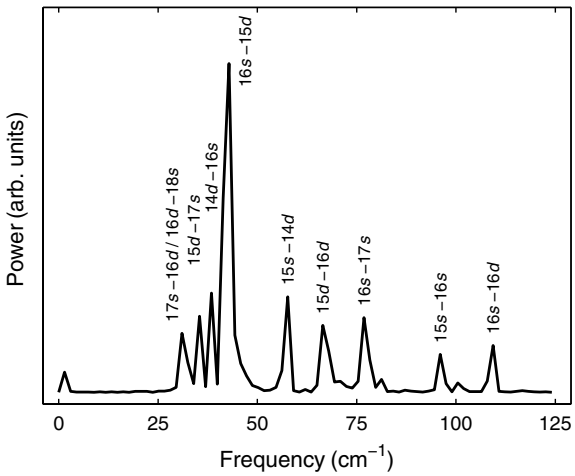

Fig. 5. Power spectrum of the $\pi^2 \parallel \pi$ trace in Figure 4.

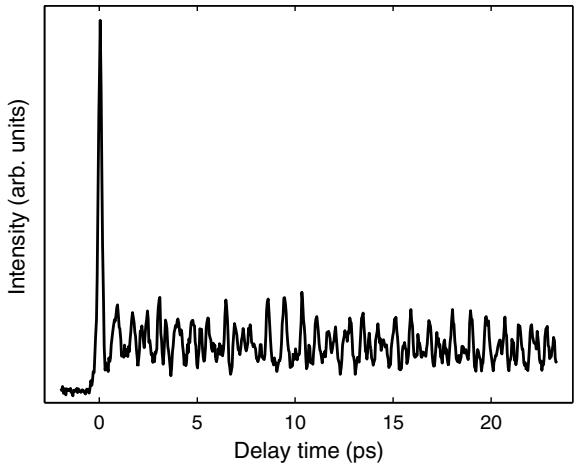

Fig. 6. Time trace obtained with the $\pi^2 \perp \pi$ scheme and $\lambda_{pu} = 411\,\text{nm}$ and $\lambda_{pr} = 837\,\text{nm}$.

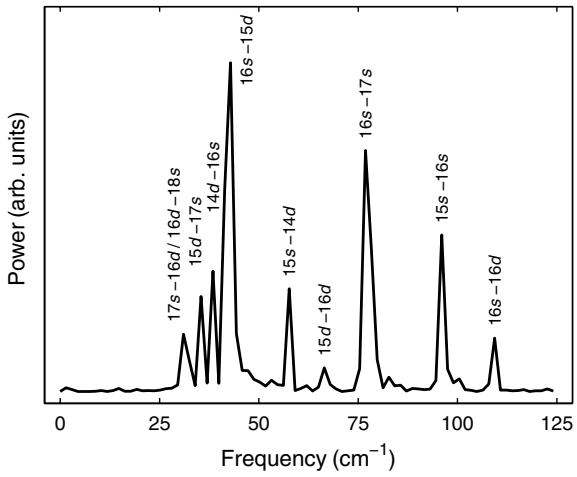

Fig. 7. Power spectrum of the $\pi^2 \perp \pi$ trace in Figure 6.

A strong $t = 0$ peak is found with all pump-probe schemes. Likely, it arises from a collection of complicated light-matter interactions when the two pulses overlap in time and dies away as the pulses separate similarly to the in ultrafast spectroscopy often-called coherent artefact [19]. The extension of this coherent spike demarcates a region in which our theoretical expressions above do not hold.

Finally, weak decay of the overall signal intensity, in this case with a time constant in the order of 10 ps, is to varying extent observed in all traces. It is most likely due to atomic decoherence induced by residual collisions with the buffer gas.

4.2 Linear light polarization

Clearly, the $\pi^2\pi$ scheme should be expected to produce more complicated superposition states than the one involving circular light polarization. The quantum beat structures in Figures 4 and 6 indeed look more involved than the previous one. This is also reflected in the respective power spectra in Figures 5 and 7 displaying a multitude of beats of three different kinds — *s*-*s*, *d*-*d*, and *s*-*d*.

The variation in amplitudes of the frequency peaks in the parallel and perpendicular polarisation schemes reflects the rank of the corresponding beat term in equation (7) and may thus be used to extract information on the symmetry of each frequency component. Most notably, as done below, the isotropic and anisotropic contributions to the signal can be separated from each other.

5 Discussion

We wish here to assess the validity of the KC conjecture with respect to pulsed pump-probe spectroscopy. The conjecture concerns the existence of isotropic pure n-manifold quantum beats and we proceed by first evidencing the existence of precisely such beats in our measured signal. Secondly, we present a physical interpretation of these quantum beats within the coupled-uncoupled state formalism.

5.1 Analysis – existence of isotropic quantum beats

Generally spoken, our spectra reflect truthfully the calcium energy level structure [16] in that the observed beat frequencies correspond to essentially all relevant combinations of levels. The noteworthy exception to this is that peaks involving the $4s13d$ and $4s14d$ levels are consistently weaker than the other ones, in the former instance to the extent that they are unobservable. This presumably is a consequence of spin-orbit perturbation of these levels [16].

The existence of pure n-manifold quantum beats, in our case beats of s-s and d-d type, is most directly addressed by the $[\sigma^+]^2\sigma^-$ scheme. Requiring $m_J = 2$ in the intermediate state, it allows excitation of only the $(4snd)\,^1\mathrm{D}_2$ manifold which implies that all states $|j\rangle$ have identical angular momentum quantum numbers. Evidently, from Figures 2 and 3 there are beats present in this case and they are indeed only of the d-d kind. Further evidence for the existence of pure n-manifold beats are found by inspection of the spectra obtained with the $\pi^2\pi$ scheme. Both Figures 5 and 7 contain in addition to d-d beats also s-s beat frequencies.

A characteristic feature of pure n-manifold beats, as argued above, is that they should be isotropic. That is, in the $\pi^2\pi$ scheme their amplitude should not depend on the relative orientations of the pump and probe polarizations. All other kinds of beats would be anisotropic. The two symmetry classified contributions to our signal can be separated by the standard formula for light anisotropy [15]

$$R(t) = \frac{I_{\parallel}(t) - I_{\perp}(t)}{I_{\parallel}(t) + 2I_{\perp}(t)}, \tag{9}$$

where $I_{\parallel}(t)$ and $I_{\perp}(t)$ is the signal obtained with the $\pi^2 \parallel \pi$ and $\pi^2 \perp \pi$ scheme, respectively. It is readily found that $R(t)$ contains contributions from only the $k_3 = 2$ terms in equation (5) whereas the denominator is isotropic, that is, it corresponds to the $k_3 = 0$ part.

The anisotropy power spectrum obtained from $R(t)$ is shown in Figure 8. Note that within experimental uncertainty only mixed s-d type of beats and no s-s or d-d beats are seen. The latter beats reappear, however, in the spectrum of the isotropic part (not shown) in which there are no s-d frequencies present. We conclude that the observed pure n-manifold quantum beats indeed are isotropic, in compliance with equation (5).

5.2 Interpretation – coupled-uncoupled state representation of quantum beats

Our experimental results thus showed clear evidence of isotropic quantum beating. By inference, the corresponding zero rank terms in equations (4) and (5) describing pump-probe signals cannot denote simply the population number of excited atoms as frequently interpreted [8]. We formulate here a more adequate physical interpretation within the coupled-uncoupled quantum states formalism recently investigated in connection with coherent population trapping [20,21] and quantum beating in atomic

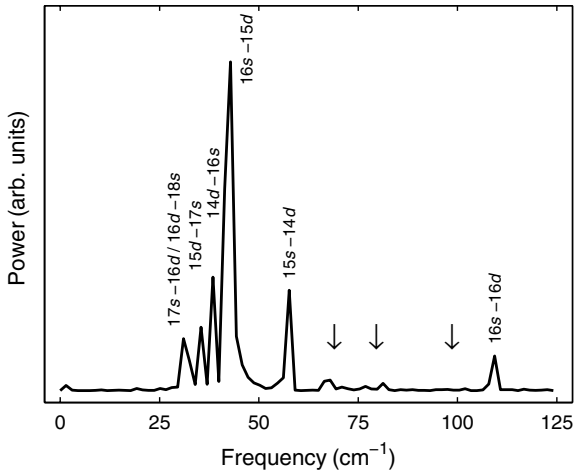

Fig. 8. Power spectrum of $R(t)$ formed from the traces in Figures 4 and 6. Arrows mark expected positions of s-s and d-d beats from Figures 5 and 7.

photoionisation [22]. This formalism is a non-perturbative one, that is, it does not contain the perturbation theory expressions describing interaction of atoms with radiation like in equation (3).

Considering excitation of atoms from the ground to the excited states in the pump-probe experiment we will for clarity restrict ourselves to one-photon transitions. For $t \geq \tau$ the total time-dependent atomic wavefunction $|\Psi(t)\rangle$ can in general be expanded over the time-independent basis as

$$|\Psi(t)\rangle = \sum_k a_k(t)\,|k\rangle\,, \tag{10}$$

where $a_k(t)$ is a probability amplitude and the index k runs over all quantum states involved in the process. Describing interaction of the atom with the pump and probe pulses separately, we consider the simplest case of a four-level atom with one ground $|g\rangle$, two intermediate $|1\rangle$, $|2\rangle$, and one final $|f\rangle$ quantum state. The external electromagnetic field will be treated classically. The amplitudes $a_k(t)$ are subject to the Schrödinger equation which in the rotating wave approximation for the pump process can be written

$$\begin{aligned} i\frac{\partial}{\partial t}a_g &= \omega_g a_g - \frac{1}{\hbar}E^*_{pu}\tau_{pu}\,\delta(t-t_0)\sum_{j=1}^{2}\langle g|\,\mathbf{de}^*_{pu}\,|j\rangle\,a_j, \\ i\frac{\partial}{\partial t}a_j &= \omega_j a_j - \frac{1}{\hbar}E_{pu}\tau_{pu}\,\delta(t-t_0) \\ &\quad\times\langle j|\,\mathbf{de}_{pu}\,|g\rangle\,a_g, \quad j=1,2. \end{aligned} \tag{11}$$

where E_{pu} is the pump field amplitude, τ_{pu} is a pump pulse duration, and the δ-function $\delta(t-t_0)$ represents the pump pulse at time t_0. The frequencies ω_1, ω_2, and ω_g are atomic level frequencies, $\omega_k = E_k/\hbar$. Similar equations can be written for the probe process.

When the pump pulse duration is much smaller than the inverse frequency separation between the intermediate states $|1\rangle$ and $|2\rangle$, $\tau_{pu} \ll \omega_{12}^{-1}$, the frequencies ω_1 and ω_2 in

equation (11) can be taken equal to each other. It then can be shown from equation (11) that the pumping field can couple the ground state only to a particular superposition of the excited states

$$|c\,pu\rangle = D_{pu}^{-1}\Big(|1\rangle \langle 1|\,\mathbf{de}_{pu}\,|g\rangle + |2\rangle \langle 2|\,\mathbf{de}_{pu}\,|g\rangle \Big) \quad (12)$$

where $D_{pu} = \left(\sum_{j=1}^{2} |\,\langle g|\,\mathbf{de}_{pu}^{*}\,|j\rangle\,|^2\right)^{1/2}$ is a normalization factor. The corresponding probability amplitude is

$$a_{c\,pu} = D_{pu}^{-1}\Big(\langle g|\,\mathbf{de}_{pu}^{*}\,|1\rangle\, a_1 + \langle g|\,\mathbf{de}_{pu}^{*}\,|2\rangle\, a_2\Big). \quad (13)$$

The orthogonal superposition state $|nc\,pu\rangle$ and the corresponding probability amplitude $a_{nc\,pu}$ can be found as

$$|nc\,pu\rangle = D_{pu}^{-1}\Big(-|1\rangle \langle g|\,\mathbf{de}_{pu}^{*}\,|2\rangle + |2\rangle \langle g|\,\mathbf{de}_{pu}^{*}\,|1\rangle \Big) \quad (14)$$

$$a_{nc\,pu} = D_{pu}^{-1}\Big(-\langle 2|\,\mathbf{de}_{pu}\,|g\rangle\, a_1 + \langle 1|\,\mathbf{de}_{pu}\,|g\rangle\, a_2\Big). \quad (15)$$

This state remains uncoupled with the ground state and acquires no population during the pumping pulse.

Coupled and uncoupled states with respect to the probe pulse $|c\,pr\rangle$, $|nc\,pr\rangle$ can be defined in a similar way.

Transformation from the basis $|j\rangle = |1\rangle\,, |2\rangle$ to the basis $|c\,\rangle, |nc\,\rangle$ according to equations (12) and (14) is unitary thus leading to equivalent expressions for the signal. This transformation greatly simplifies the system of three coupled equations in equation (11) reducing it to a system of two coupled equations for the amplitudes a_g and $a_{c\,pu}$

$$\begin{aligned} i\frac{\partial}{\partial t}a_g &= \omega_g a_g - \frac{1}{\hbar} D_{pu} E_{pu}^{*} \tau_{pu}\, \delta(t - t_0)\,, \\ i\frac{\partial}{\partial t}a_{c\,pu} &= \omega_1 a_{c\,pu} - \frac{1}{\hbar} D_{pu} E_{pu} \tau_{pu}\, \delta(t - t_0)\, a_g \end{aligned} \quad (16)$$

and one decoupled equation for $a_{nc\,pu}$

$$i\frac{\partial}{\partial t}a_{nc\,pu} = \omega_1 a_{nc\,pu} \quad (17)$$

which easily can be solved analytically.

In the absence of the laser radiation the atomic system evolves according to the purely atomic Hamiltonian $\hat{H}_a$ as shown in equation (2) with the $|j\rangle = |1\rangle$ and $|2\rangle$ eigenstates. The explicit set of equations for this case is

$$\begin{aligned} &i\frac{\partial}{\partial t}a_g = 0, \\ &i\frac{\partial}{\partial t}a_1 = \omega_1 a_1, \quad i\frac{\partial}{\partial t}a_2 = \omega_2 a_2. \end{aligned} \quad (18)$$

Note that in the latter equation we make distinction between ω_1 and ω_2, since, unlike the pulse duration τ, the time interval t between the pump and probe pulses is comparable to or larger than ω_{21}^{-1}.

Consecutively solving equations (16) and (18) together with the similar set of equations for the probe laser pulse, the expression for the pump-and-probe signal finally becomes

$$I(t) \sim \Bigg| (D_{pu} D_{pr})^{-1} \sum_{j=1}^{2} \langle f|\,\mathbf{de}_{pr}^{*}\,|j\rangle \langle j|\,\mathbf{de}_{pu}\,|g\rangle + 2\,\mathrm{Re}\,\left(\langle f|\,\mathbf{de}_{pr}^{*}\,|2\rangle \langle 1|\,\mathbf{de}_{pu}\,|g\rangle\, e^{i\omega_{21}t}\right)\Bigg|^2 \quad (19)$$

where $\mathbf{e}_{pr}$ and D_{pr} is the probe pulse polarization vector and the corresponding dipole matrix element, respectively.

The interference term in equation (19) displays beating at the frequency ω_{21}. These beats are definitely isotropic because no angular momenta of the atom were introduced into our simple four-level model. Moreover, they have clear physical meaning, as the excited state population oscillates between the coupled and uncoupled states defined with respect to the probe pulse.

In fact, equation (19) corresponds to the $K = 0$ term in equation (4). The equation can be easily generalized, however, to the case of degenerate quantum states $|nLM\rangle$. Consideration of more than two intermediate states $|j\rangle$ leads only to an increase in the number of coupled-uncoupled states, while for every pulse, pump or probe, these states can be defined in the same way. As a result the generalized equation (19) becomes equivalent to equation (4). Thus, the advantage of using the coupled and uncoupled basis states is just the clarity of physical picture. Note, however, the interpretation presented here is not a perturbative approach that drops higher-order contributions. Thus, the occurrence of isotropic beats in the theoretical signal cannot be associated with an incorrect series truncation, as inferred by the KC conjecture [9–11].

It should be noted that if the pulse duration is comparable to the inverse frequency separation between the excited states $|j\rangle$, but small compared to the natural lifetimes of the excited states, the coupled and uncoupled states formalism still can be used. In such a case, these states must be defined with respect to the S-matrix describing evolution of an atom under the action of an electromagnetic radiation pulse of finite duration.

As shown above, our experimental results and their theoretical interpretation do not support the *general* KC conjecture [12] — that is, we do observe in pump-probe experiments quantum beats between states differing only in principal quantum number and, moreover, the beats can be explained by a non-perturbative, coupled-uncoupled states model. Careful analysis of the arguments of Khvostenko et al. in references [8–11], however, shows that the theory as developed there pertains only to a single photon scattering by an atom, the results meaning that the total cross-section of a photon scattering event displays no net interference of paths via various excited levels having the same angular quantum numbers and different principal quantum numbers. As known from quantum electrodynamics (see, e.g., the monograph [23]), the radiation field states with definite photon numbers (Fock states) considered by KC have indefinite phase value and do not reflect the properties of the classical

electromagnetic field generated by lasers. The latter field can be modelled only by photons in coherent quantum states with large mean photon numbers.

The formalism of coupled and uncoupled states used in this paper, on the other hand, is applicable only to the case of irradiation of an atom by classical electromagnetic fields [20] and is not appropriate for treating of photon Fock states.

Therefore, as our experimental results and theoretical interpretation are obtained for classical electromagnetic fields they are strictly speaking not in contradiction with the result of the theory developed by Khvostenko and coworkers in references [8–11]. The properties of the nonclassical photon states are so far rather scarcely investigated experimentally and direct verification of the results of the KC theory using single mode photon Fock states would be of great interest.

6 Conclusion

Summing up, our experiments show clear evidence of isotropic quantum beating generated by atomic states with all angular momenta and their projections equal. The theoretical analysis explains the experimental result within the coupled-uncoupled states picture and shows that the standard formula (3) is valid for all possible values of L and L', contrary to the prediction of the general KC conjecture. Our results are strictly valid for a pump-probe detection scheme and for classical electromagnetic fields.

In a forthcoming publication we intend to report on studies of isotropic quantum beating induced by a short light pulse and detected by time-resolved fluorescence.

This work was supported by the RFBR grant No. 02-03-32914, RFBR grant No. 02-02-17686, Russian Leading Scientific Schools 1115.2003.2, and the Swedish Research Council (VR).

References

1. E.B. Alexandrov, Opt. Spectrosc. **18**, 522 (1964)
2. J.N. Dodd, R.D. Kaul, D.M. Warrington. Proc. Phys. Soc. Lond. **84**, 176 (1964)
3. H. Bitto, J.R. Huber, Opt. Commun. **80**, 184 (1990)
4. S. Savikhin, D.R. Buck, W.S. Struve, Chem. Phys. Lett. **223**, 303 (1997)
5. H.J. Andrä, Phys. Rev. Lett. **25**, 325 (1970)
6. T. Hadeishi, W.A. Nierenberg, Phys. Rev. Lett. **14**, 891 (1965)
7. *The physics and chemistry of wave packets*, edited by J. Yeazell, T. Uzer (Wiley, 2000)
8. E.B. Alexandrov, M.P. Chaika, G.I. Khvostenko, *Interference of atomic states* (Springer, 1993)
9. G.I. Khvostenko, Opt. Spectrosc. **71**, 506 (1991)
10. G.I. Khvostenko, M.P. Chaika, Opt. Spectrosc. **53**, 972 (1982)
11. G.I. Khvostenko, M.P. Chaika, Opt. Spectrosc. **59**, 714 (1982)
12. G.I. Khvostenko, Opt. Spectrosc. **78**, 1 (1995)
13. M. Strehle, U. Weichmann, G. Gerber, Phys. Rev. A **58**, 450 (1998)
14. D.A. Varshalovich, A.N. Moskalev, V.K. Khersonskii, *Quantum Theory of Angular Momentum* (World Scientific, 1988)
15. R.N. Zare, *Angular Momentum* (Wiley, 1988)
16. J.A. Armstrong, P. Esherick, J.J. Wynne, Phys. Rev. A **15**, 180 (1977)
17. J.A. Armstrong, J.J. Wynne, P. Esherick, J. Opt. Soc. Am. **69**, 211 (1979)
18. T. Feurer, A. Glass, R. Sauerbrey, Appl. Phys. B: Lasers Opt. **65**, 295 (1997)
19. S. Mukamel, *Nonlinear Optical Spectrocscopy* (Oxford, 1995)
20. B.D. Agap'yev, M.B. Gornyi, B.G. Matisov, Yu.V. Rozhdestvenskii, Uspekhi Fiz. Nauk. **163**, 1 (1993)
21. E. Arimondo, Progr. Opt. **35**, 257 (1996)
22. S. Zamit, M.A. Bouchene, E. Sokell, C. Nicole, V. Blanchet, B. Girard, Eur. Phys. J. D **12**, 255 (2000)
23. R. Loudon, *The quantum theory of light*, 2nd edn. (Oxford University Press, 1983)